Dynamic Fracture in Single Crystal Silicon

Jens A. Hauch, Dominic Holland, M. P. Marder, and Harry L. Swinney

Center for Nonlinear Dynamics and Department of Physics

The University of Texas at Austin, Austin, TX 78712

(February 1, 2008)

We have measured the velocity of a running crack in brittle single crystal silicon as a function of energy flow to the crack tip. The experiments are designed to permit direct comparison with molecular dynamics simulations; therefore the experiments provide an indirect but sensitive test of interatomic potentials. Performing molecular dynamics simulations of brittle crack motion at the atomic scale we find that experiments and simulations disagree showing that interatomic potentials are not yet well understood.

PACS numbers: 62.20.Mk, 02.70.Ns, 34.20.Cf

Data on fracture in single crystals are limited due to the difficulties in performing precisely controlled experiments. There is also a lack of atomic scale simulations that allow quantitative comparison with fracture experiments. We have obtained both experimentally and numerically the velocity v of a crack propagating in a silicon single crystal as a function of the energy flux to the crack tip, the fracture energy G. The relation between v and G is very sensitive to crystal structure and details of interatomic forces. Thus the experimentally determined $v(G)$ provides a test of the interatomic potentials used in simulations. We find poor quantitative agreement between simulation and experiment, showing that the existing potentials do not capture the complexities of fracture.

Experiments – We chose silicon for our experiments since it is very brittle at room temperature [1] and readily available as oriented single crystals. The lowest energy cleavage plane in silicon is the {111} plane. All experiments reported here were performed on p-type {110} wafers (0.38 mm thick) with a doping level of $\sim 10^{19}$ boron atoms per cm^3; {110} wafers are the only commercially available wafers with a {111} plane normal to the plane of the wafer.

Previous experiments in single crystal silicon [2–4] measured the minimum energy density required to drive a crack, and a few have measured dynamic crack behavior [5,6], but without the ability to measure the fracture energy. In our experiments samples were loaded in a thin strip configuration by displacing the edges of the wafer a constant amount δ, as shown in Fig. 1 (b). Thin strip refers to samples with an aspect ratio $L/W > 1$. In all experiments described here, $L = 7.5$ cm and $W = 3.3$ cm, giving an aspect ratio of 2.3. The advantage of this tensile loading geometry is that if the boundaries of the sample can be held fixed while the crack propagates, then the energy released to the crack tip is independent of crack length and results in steady state fracture at constant velocity [7–9]. In this loading configuration, G is simply the elastic strain energy stored per unit area (xz-plane in Fig. 1 (a)) ahead of the crack, and can be written as a simple function of the sample width W, width extension

δ, Young's modulus E, and for very thin samples, giving plane stress conditions, Poisson's ratio ν:

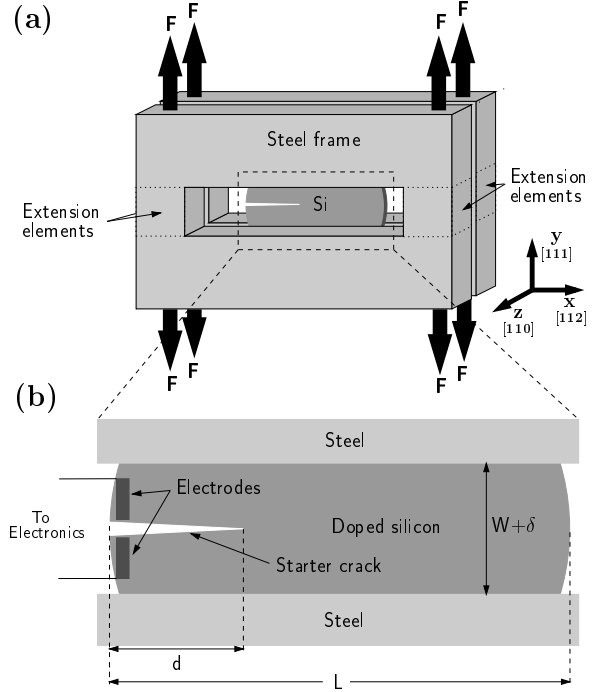$$G = \frac{1}{2} \frac{E}{1 - \nu^2} \frac{\delta^2}{W}. \tag{1}$$

FIG. 1. (a) Rigid jaw loading configuration. The steel frames are loaded symmetrically with a constant force at 8 points. This causes a small extension of the extension elements, leading to a small displacement δ of the inside edges of the frame. (b) A wafer in the frame. The extension of the frame enforces constant displacement boundary conditions on the wafer.

To open a crack along a {111} plane, δ must be about 1 μm ($E_{111} = 188$ GPa, ν=0.272 [10], $G = 2.4$ J/m^2 [11]). In a controlled experiment δ has to be maintained constant along the whole length of the wafer. The control required to maintain small, constant displacements

is difficult to achieve in a conventional tensile testing machine because as a sample fractures, the force it exerts on the testing machine decreases and the machine responds rapidly enough to affect the crack dynamics. This effect is independent of the stiffness of the testing machine [12]. Therefore we designed the frame loading configuration shown in Fig. 1 (a). It consists of two steel frames with a rectangular hole milled out of each. In an experiment, the silicon sample is clamped and glued with slow curing cyanoacrylate adhesive between the two frames, exposing a thin strip in the hole. When loaded, the frames act as two rigid bars connected by two extension elements which function as very stiff springs.

To extend the extension elements by 1 μm requires a loading force of about 8000 N distributed over the eight loading points. The extension pulls apart the inside edges of the hole, which in turn enforces a constant displacement on the edges of the silicon wafer. Fracture of the sample does not lead to a relaxation of the frame, since only a small fraction ($< 2\%$) of the total load is transmitted through the silicon sample. One concern, however, is non-ideal deformation of the rigid frame itself. Finite element analysis of the sample and frame shows that the total displacement of the edges of the wafer is constant to within 10% along the length of the sample.
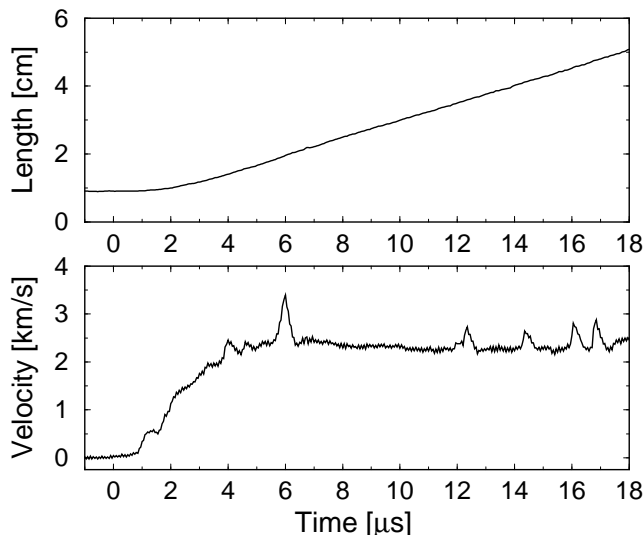

FIG. 2. Full length and velocity record for a break in silicon along the $\{111\}$ plane in the $[\bar{1}\bar{1}2]$ direction at a fracture energy of $5.08 \, \text{J/m}^2$. The velocity peaks that are visible are probably the result of acoustic waves, generated by the crack initiation, interacting with the crack tip.

To obtain fracture along a $\{111\}$ plane, it is necessary to start with a seed crack in this plane. The seed crack is formed by a thermal shock technique involving three steps. First, the sample is notched with a diamond disc saw. Next, the sample is heated by dipping it partially into boiling water. Finally, the hot sample is rapidly lowered to the desired seed crack length (1 to 3 cm) into

ice-water so that the thermal stresses induced in the sample provide an opening force perpendicular to the $\{111\}$ plane, resulting in a sharp seed crack. Length and sharpness of the seed crack determine the failure stress of the sample. Therefore by varying the seed crack length it is possible to get cracks to propagate at different fracture energies.

To measure crack length and velocity during crack propagation, a potential-drop technique similar to the one outlined in ref. [12] was used. Potential-drop techniques monitor the change in resistance of a conductor, in this case doped silicon, during crack propagation. Resistance was measured by attaching electrodes on both sides of the seed crack as shown in Fig. 1 (b). The electrodes were then connected to a Wheatstone bridge. To interpret the data, a lookup table of resistance as a function of crack length was created. The bridge output was digitized at 10 MHz (12 bit), leading to a resolution of about 1 mm in crack length. To attain good resolution of the velocity, the output of the bridge was fed into an analog differentiator and digitized at 20 MHz (8 bit). With this method the velocity measurements were limited by noise to a resolution of 50 m/s. A full data set obtained by this method is shown in Fig. 2. The data show that after an initial acceleration stage, the crack velocity settles into a steady value of 2.3 ± 0.3 km/s. The experimentally observed crack velocities range from $\simeq$40-75% of the transverse sound speeds in silicon in agreement with previously observed crack velocities [13].
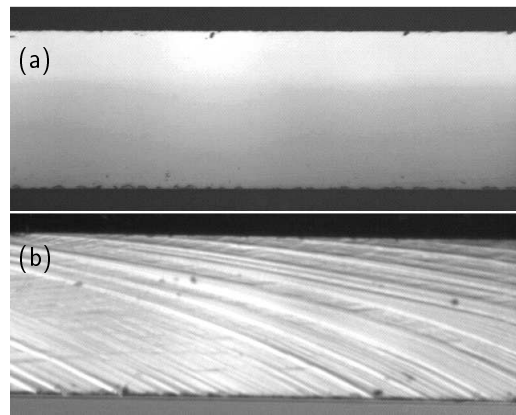

FIG. 3. (a) Featureless fracture surface resulting from uniform loading; (b) surface structure resulting from bending of the sample during the experiment. The region shown is 1.6 mm $\times$ 0.38 mm.

Samples were loaded quasi-statically by incrementing δ by about 0.03 μm at intervals of 60 s. The majority of experimental attempts had to be discarded because nonuniform curing of the adhesive caused the wafers to bend slightly out of plane during loading, so that the samples were twisted, not just stretched. Such wafers were easily identified by examining the surface created

2

by the passing crack. If a bending moment existed during fracture, the crack would leave behind structure on the fracture surface, as shown in Fig. 3 (b). Under these conditions Eq. (1) would not apply and all the samples that displayed these markings were eliminated, while only samples that showed a perfect mirror-smooth fracture surface, as shown in Fig. 3 (a), were kept. The plot of average crack velocity as a function of fracture energy for all the remaining samples is shown in Fig. 4.
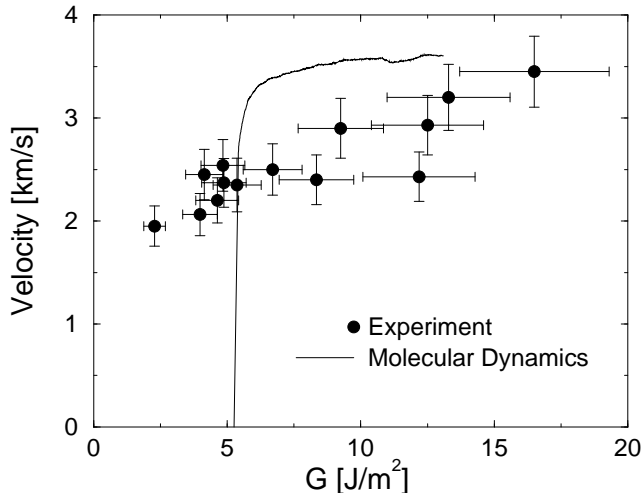

FIG. 4. Crack velocity as a function of fracture energy from experiments and molecular dynamics simulations at 300 K. The error bars in the experiments are the result of random errors due to variations in sample resistivity, while the uncertainty in the fracture energy is systematic and the result of uncertainty in the strain obtained from strain gage measurements. All low-lying velocity states exist in the simulations for temperatures down to about 200 K.

Simulations – We have also carried out molecular dynamics simulations of fracture in silicon, the results of which are also shown in Fig. 4. The simulations are carefully designed to measure numerically the same quantities measured in experiments, despite the great difference in scale between them. Since the experiments are performed at room temperature, the simulations were also maintained at 300 K by contact with a heat bath. These simulations, which are described in Ref. [8,14], use a modified Stillinger-Weber interatomic potential. The original Stillinger-Weber potential [15], like the more sophisticated environment-dependent interatomic potential [16,17], did not yield brittle crack propagation. Most potentials for silicon, of which there are over 30 [18], have a range restricted to nearest neighbors, $\simeq 3.5$ Å, although density functional theory predicts a range of $\simeq 5.5$ Å. Because of the short cutoff, potentials must rise from the cohesive well and go to zero rapidly, resulting in an unreasonably large force of attraction before rupture. This large force inhibits crack propagation: the seed crack tip blunts and will not move; at

very high strains, the tip simply melts. Without changing the form of the Stillinger-Weber potential, we were able to get cracks propagating along the experimentally preferred fracture planes, {111} and {110}, simply by doubling the strength of the term enforcing fixed angles between bonds. With this modified potential, it is possible to observe brittle fracture and calculate the relation between crack velocity v and fracture energy G. While this modification does not affect the Griffith point and makes a quantitative comparison to the experiments possible the changed potential cannot be regarded as superior to the original Stillinger-Weber potential since some of the material properties are changed. The modification changes the melting temperature from $\simeq 1400$ K to $\simeq 3500$ K compared to $\simeq 1685$ K for real silicon. The elastic properties are also affected by the modification; for example Young's modulus along the [111] direction is changed from $E_{111} = 151$ GPa to $E_{111} = 207$ GPa for the modified potential, while experimentally $E_{111} = 188$ GPa. Improved interatomic potentials are clearly needed.

The results from simulations presented in Fig. 4 were obtained for a thin strip of size $532 \times 15 \times 154$ Å^3, periodic along the thin axis. New material was added ahead of the crack tip and old material lopped off at the tail every time the crack advanced to within 200 Å of the forward end of the strip. In this fashion, the crack traveled 7 μm during the course of the simulations as G was varied between 5 and 14 J/m^2.

Comparison – The highest crack velocities observed in Fig. 4 are reasonably close, but the minimum fracture energies at which a crack propagates differ: 2.3 J/m^2 in the experiments and 5.2 J/m^2 in the simulations. Since the scale of crack velocities in a material is bounded by sound speeds [19], which potentials get approximately right, it is not surprising that the experimental and computational crack velocity scales agree. Furthermore, the potential gives the correct cohesive energy of silicon, leading to the agreement in numerical and experimental energy scales. However, the nonlinear parts of the potential involved in stretching and rupturing bonds play an important role in determining the actual fracture energies and crack velocities, in particular where the crack arrests and what its highest velocity is. The quantitative disagreements we find point to a shortcoming of the nonlinear parts of the potential, which have not received much attention.

The lowest fracture energy at which a crack propagated in the experiments was close to the lower bound estimate of the fracture energy for a {111} plane, 2.2 J/m^2 [11], which is twice the surface energy density. Since a crack cannot travel with less energy, there must be a narrow range of fracture energy over which the crack velocity rises rapidly from zero to the lowest value measured, $\simeq 2$ km/s. This phenomenon is also seen in glass and polymers and is reminiscent of a velocity gap in the lattice models of Marder et al. [20] and in simulated systems

[8,9]. A velocity gap is a band of velocities in which it is impossible for a crack to travel in steady state. In our numerical silicon, the velocity gap is temperature dependent, vanishing above 200 K. At 300 K there do exist steady states at all velocities between 0 and 3 km/s.

Steady state experiments are difficult in the narrow range of fracture energy where $v(G)$ rises sharply because of the extreme precision required at the boundaries. However, in glass and Plexiglas it was possible to rule out the existence of a velocity gap by conducting carefully controlled crack arrest experiments, which showed, by slowly decreasing the energy flux to the crack tip, that all velocities are available to the crack [12]. A velocity gap should show up as a very rapid velocity jump between zero and roughly 20-40% of the sound speed at initiation. The accelerations observed in the experiments can be compared to the timescales available to the system through the nondimensional acceleration $\bar{a} = aW/c^2$, where c is the sound velocity, W the sample width, and a is the acceleration. In our experiments we routinely observe accelerations on the order of 10^9 m/s^2 in silicon, which corresponds to $\bar{a} \simeq 1$. This acceleration is not large, but due to three dimensional averaging over the whole crack front that is involved in our measurement, our data do not completely rule out the possibility of a velocity gap in silicon at room temperature.

The experiments covered a range of fracture energies, $2 - 16$ J/m^2, in which the cracks produced very smooth surfaces. Thus cracks can dissipate large amounts of energy, more than seven times the amount needed to create a clean cleavage through the whole crystal, without leaving behind any large scale damage on the fracture surfaces. Investigation by atomic force microscopy shows that for low fracture energies the fracture surface is atomically flat, while at higher energies the surface has definite features. These features are smooth on the submicron scale, and account for height variations on the order of 30 nm over an area of $16\,\mu$m^2. The roughness gives an area increase of only ~0.1% above that of a flat cleaved surface. This added surface cannot account for the sevenfold increase in dissipated energy. We do not know the mechanism by which the extra energy is dissipated. However, the computations indicate that most of it is carried off in lattice vibrations. In polymers energy is also dissipated through the creation of small microcracks, which are visible on the fracture surface in the form of a mirror-mist-hackle transition [21–23,12]. The observation of such a transition in silicon [6] implies that a similar mechanism may be important in silicon as well.

Conclusions – We have measured the dependence of crack velocity on fracture energy in single crystal silicon. We control the velocity of a running crack by controlling the energy flux to the crack tip. Experiments and simulations agree qualitatively, for both show an initial sharp rise in velocity, followed by slowly increasing crack velocities as fracture energy increases. However, details

in the relation between v and G are quite sensitive to details of interatomic potentials. The ability to compare experiment and computation provides a strong test of potentials, but the quantitative disagreement we find demonstrates that they are not yet correct.

[1] B. Lawn, *Fracture in Brittle Solids*, 2nd ed. (Cambridge University Press, Cambridge, 1975).
[2] F. Ericson and J. Schweiz, J. Appl. Phys. **68**, 5840 (1990).
[3] J. J. Gilman, J. Appl. Phys. **31**, 2208 (1960).
[4] C. P. Chen and M. H. Leipold, Am. Cer. Soc. Bull. **59**, 469 (1980).
[5] M. Brede, K. J. Hsia, and A. S. Argon, J. Appl. Phys. **70**, 758 (1991).
[6] T. Cramer, A. Wanner, and P. Gumbsch, Phys. Stat. Sol. **164**, R5 (1997).
[7] J. C. Rice and W. G. Knauss, J. Appl. Mech. - Trans. of the ASME **89**, 249 (1967).
[8] D. Holland and M. P. Marder, Phys. Rev. Lett. **80**, 746 (1998).
[9] P. Gumbsch, S. J. Zhou, and B. L. Holian, Phys. Rev. B **55**, 3445 (1997).
[10] W. A. Brantley, J. Appl. Phys. **44**, 534 (1972).
[11] J. C. H. Spence, Y. M. Huang, and O. Sankey, Act. Met. Mat. **41**, 2815 (1993).
[12] J. A. Hauch and M. P. Marder, Int. J. Frac. **90**, 133 (1998).
[13] J. E. Field, Cont. Phys. **12**, 1 (1971).
[14] D. Holland and M. Marder, Phys. Rev. Lett. **81**, 4029 (1998).
[15] F. H. Stillinger and T. A. Weber, Phys. Rev. B **31**, 5262 (1985).
[16] M. Z. Bazant, E. Kaxiras, and J. F. Justo, Phys. Rev. B **56**, 8542 (1997).
[17] J. Justo *et al.*, Phys. Rev. B **58**, 2539 (1998).
[18] H. Balamane, T. Halicioglu, and W. A. Tiller, Phys. Rev. B **46**, 2250 (1992).
[19] L. B. Freund, *Dynamic Fracture Mechanics* (Cambridge University Press, New York, 1990).
[20] M. Marder and S. P. Gross, J. Mech. Phys. Sol. **43**, 1 (1994).
[21] E. Sharon, S. P. Gross, and J. Fineberg, Phys. Rev. Lett. **74**, 5146 (1995).
[22] E. Sharon, S. P. Gross, and J. Fineberg, Phys. Rev. Lett. **76**, 2117 (1996).
[23] K. Ravi-Chandar and W. G. Knauss, Int. J. Frac. **26**, 141 (1984).